Reviews in Cardiovascular Medicine

Rev. Cardiovasc. Med. **2026**; 27(2): 42804
https://doi.org/10.31083/RCM42804

Original Research

Targeting Tumor Necrosis Factor-α Mitigates Glucose Fluctuation-Induced Aortic Valve Fibrosis: Insights From Diabetic Rat Models

Yu-Jia Chen[1,†], Hui-Ping Chen[2,†], Chang-Ying Zhang[1], Xiao-Song Rong[3], Ku-Lin Li[1], Feng Xiao[1,*], Ru-Xing Wang[1,*]

[1]Department of Cardiology, The Affiliated Wuxi People's Hospital of Nanjing Medical University, Wuxi People's Hospital, Wuxi Medical Center, Nanjing Medical University, 214023 Wuxi, Jiangsu, China
[2]Department of Cardiology, Taizhou Second People's Hospital Affiliated to Yangzhou University, 225500 Taizhou, Jiangsu, China
[3]Department of Cardiovascular Surgery, The Affiliated Wuxi People's Hospital of Nanjing Medical University, Wuxi People's Hospital, Wuxi Medical Center, Nanjing Medical University, 214023 Wuxi, Jiangsu, China
*Correspondence: xiaofeng@njmu.edu.cn (Feng Xiao); ruxingw@aliyun.com (Ru-Xing Wang)
†These authors contributed equally.
Academic Editor: Carmela Rita Balistreri
Submitted: 1 June 2025 Revised: 24 October 2025 Accepted: 28 October 2025 Published: 13 February 2026

Abstract

Background: Calcific aortic valve disease (CAVD) is a progressive condition characterized by inflammation and fibrous calcification remodeling, with aortic valve fibrosis (AVF) representing the associated subclinical phase. Early intervention with oral medication during the AVF stage may prevent and slow the development and progression of CAVD. Previous studies have demonstrated that individuals with diabetes are at an elevated risk of CAVD and also experience a significantly higher incidence of aortic valve stenosis, which rapidly advances from mild to severe stages. Significantly, the adverse effects of glucose fluctuations (GFs) on cardiovascular diseases exceed those associated with persistent hyperglycemia. Nonetheless, the mechanisms through which GFs contribute to AVF, the early stage of CAVD, remain inadequately understood. Consequently, this study aimed to investigate the inflammatory mechanisms underlying AVF induction in response to fluctuations in glucose levels. **Methods**: Diabetic rat models were established through intraperitoneal injection of streptozotocin (STZ). GFs in these diabetic rats were managed by alternating between a Western diet and periods of fasting. Infliximab was administered to inhibit inflammation mediated by tumor necrosis factor-alpha (TNF-α). For the *in vivo* study, echocardiographic assessments of the aortic valve and left ventricular function were conducted on the diabetic rats after eight weeks. Aortic valves from various groups of rats were dissected to test fibrosis, extracellular matrix remodeling, and variations in inflammatory factors, which were examined using hematoxylin and eosin (HE) staining, modified Movat–Russell pentachrome staining, and immunohistochemical staining, respectively. For the *in vitro* study, porcine valvular interstitial cell (VIC) cultures were used to establish GF-induced fibrosis, thereby elucidating the underlying inflammatory mechanisms. **Results**: Our study demonstrated that GFs exacerbate AVF and dysfunction in diabetic patients. This is characterized by increased peak blood flow velocity and peak cross-valve gradient of the aortic valve. Furthermore, we observed intensified TNF-α-mediated inflammatory responses, characterized by the upregulation of T lymphocytes and macrophages, as well as activation of the Janus kinase 1 (JAK1)/signal transducer and activator of transcription 3 (STAT3) pathway. Notably, these pathological processes were ameliorated by the administration of infliximab, resulting in the downregulation of fibrotic and inflammatory markers, as well as improved echocardiographic indices. Our research findings indicate that TNF-α-mediated inflammation exacerbates fibrotic aortic valve processes through GFs, which are mediated by the JAK1/STAT3 signaling pathway. **Conclusions**: Targeting TNF-α may serve as a potential therapeutic target to mitigate the progression of inflammation-induced aortic valve damage and fibrosis.

Keywords: aortic valve fibrosis; glucose fluctuation; diabetes; tumor necrosis factor alpha; inflammation

1. Introduction

Calcified aortic valve disease (CAVD) is a progressive cardiovascular condition characterized by fibrosis and calcification of the aortic valve leaflets [1]. The pathogenesis and progression of CAVD involve a complex, cell-driven process, in which valvular endothelial cells (VECs) and valvular interstitial cells (VICs), in conjunction with their interactions with the extracellular matrix, play a pivotal role [2]. Aortic valve fibrosis (AVF), an initial pathological stage of CAVD, is distinguished by the activation of quiescent VICs, remodeling of the extracellular matrix, and the infiltration of an inflammatory response, eventually leading to aortic valve stenosis and calcification [3,4]. As calcification deposition progressively deteriorates, AVF may advance to aortic valve stenosis, heart failure, and potentially mortality [5]. The primary therapeutic intervention for CAVD includes surgical or transcatheter aortic valve replacement, both of which are associated with a substan-

tial risk of adverse events and considerable healthcare expenses [6]. Regrettably, no pharmacological interventions have currently been identified that can reverse or decelerate the progression of CAVD. Clinical trials have demonstrated that conventional cardiovascular medications, including statins and renin–angiotensin system inhibitors, are ineffective in slowing the progression of CAVD [1]. Consequently, the exploration of therapeutic targets for the early stage of CAVD, particularly AVF, constitutes a significant challenge in clinical practice that necessitates urgent attention.

Diabetes represents a longstanding public health challenge and serves as an independent risk factor for CAVD, significantly affecting individuals worldwide [4,7]. Histopathological analyses have demonstrated that individuals with both diabetes and CAVD exhibit more severe valvular calcification, accelerated disease progression, and poorer prognostic outcomes compared to those without diabetes. Experimental models exploring hyperlipidemia and hyperglycemia have consistently identified the aortic valve as the primary site impacted by these metabolic stressors [8]. In clinical practice, hyperglycemia in individuals with diabetes predominantly presents in two forms: persistent hyperglycemia and glucose fluctuations (GFs). The latter refers to the unstable condition characterized by oscillations in blood glucose levels between peak and trough values [9]. Recent research indicates that GFs have a more significant adverse effect on the cardiovascular system compared to persistent hyperglycemia [10]. Nevertheless, the precise mechanisms through which GFs contribute to cardiovascular damage are not yet fully understood. Therefore, it is hypothesized that GFs may present a greater risk to individuals with CAVD than persistent hyperglycemia.

Tumor necrosis factor-alpha (TNF-α) is a multifunctional cytokine that is integral to numerous biological processes, including cell apoptosis, survival, and proliferation. TNF-α is predominantly secreted by activated macrophages and T lymphocytes [11,12]. Infliximab, a monoclonal antibody targeting TNF-α, has been approved for the management of various chronic inflammatory diseases. Infliximab functions by binding to both soluble and transmembrane forms of TNF-α, thereby preventing their interaction with TNF receptors (TNFRs). This action effectively inhibits the release of proinflammatory cytokines, thereby mitigating the inflammatory response. Notably, TNF-α has been identified in calcified aortic valves of both human and murine origin [13]. TNF-α significantly contributes to aortic valve calcification by affecting various processes, such as exacerbating damage to VECs, promoting monocyte adhesion, and facilitating foam cell formation [14–17]. However, the specific molecular mechanisms underlying TNF-α-mediated calcification of the aortic valve remain inadequately elucidated. The Janus kinase (JAK)/signal transducer and activator of transcription (STAT) signaling pathway, a widely expressed intracellular signaling cascade, plays a crucial role in various biological processes, including cellular proliferation, differentiation, apoptosis, and immune regulation [18]. Moreover, this pathway serves as a direct mechanism for modulating gene expression in response to extracellular stimuli. Abundant studies have demonstrated a strong correlation between the persistent activation of the JAK/STAT signaling pathway and the onset of immune and inflammatory diseases, underscoring its significance as a therapeutic target for cardiovascular diseases [19–22]. A previous study has explicitly demonstrated that the JAK/STAT signaling pathway is integral in mediating inflammation, cell apoptosis, and calcification triggered by dsRNA, thereby facilitating valve calcification [23]. As a result, the JAK/STAT signaling pathway presents as a promising target for therapeutic intervention in the management of CAVD.

This study aimed to examine the impact of GFs on the progression of AVF in rats with streptozotocin (STZ)-induced diabetes, as well as the underlying mechanisms involved. The findings suggest that the activation of the JAK1/STAT3 signaling pathway, triggered by TNF-α, is a crucial factor contributing to the pathogenesis of AVF in the presence of GFs.

2. Materials and Methods

2.1 Material

Primary polyclonal rabbit antibodies against CD3 (ab16669, Abcam Plc, Cambridge, UK), CD68 (ab955, Abcam Plc, Cambridge, UK), TNF-α (ab6671, Abcam Plc, Cambridge, UK), transforming growth factor-β1 (TGF-β1; ab92486, Abcam Plc, Cambridge, UK), α-smooth muscle actin (α-SMA; ab7817, Abcam Plc, Cambridge, UK), and JAK1 (ab138005, Abcam Plc, Cambridge, UK) proteins were purchased from Abcam, UK. Additionally, primary polyclonal rabbit antibodies against collagen 1 (14695-1-AP, Proteintech Group, Inc., Chicago, IL, USA) and collagen 3 (227345-1-AP, Proteintech Group, Inc., Chicago, IL, USA) were procured from Proteintech, USA. Phospho-STAT3 (p-STAT3, 381552, Zen Bioscience, Chengdu, China) and total-STAT3 (t-STAT3, 251611, Zen Bioscience, Chengdu, China) were acquired from Zen Bioscience, China. Injectable infliximab (CN-30069V, Cilag AG, Schaffhausen, Switzerland) was sourced from Cilag AG, Switzerland. Furthermore, an improved hematoxylin–eosin (HE) staining kit (G1121, Solarbio Technology Co., Ltd., Shanghai, China) and the modified Movat–Russell pentachrome staining kit (G3700, Solarbio Technology Co., Ltd., Shanghai, China) were purchased from Solarbio, China. In addition, the concentrated SABC-POD (Mouse/Rabbit IgG) kit (SA2010, BOSTER Biological Technology Co., Ltd., Wuhan, China), DyLight 488 conjugated AffiniPure goat anti-mouse IgG (H + L) (BA1126, BOSTER Biological Technology Co., Ltd., Wuhan, China), DyLight 594 conjugated AffiniPure goat anti-rabbit IgG (H + L) (BA1142, BOSTER Biological Technology Co., Ltd.,

Wuhan, China), ethylenediaminetetraacetic acid (EDTA) antigen retrieval solution (AR0023, BOSTER Biological Technology Co., Ltd., Wuhan, China), 4′,6-diamidino-2-phenylindole (DAPI) staining solution (AR1176, BOSTER Biological Technology Co., Ltd., Wuhan, China), human TNF-α enzyme-linked immunosorbent assay (ELISA) kit (EK0525, BOSTER Biological Technology Co., Ltd., Wuhan, China), and human TGF-β1 ELISA kit (EK0513, BOSTER Biological Technology Co., Ltd., Wuhan, China) were obtained from Boster, China. The human collagen 1 ELISA kit (CSB-EL005716HU, CUSABIO BIOTECH CO., Ltd., Wuhan, China) was obtained from CUSABIO, China.

2.2 In Vitro Model of Glucose Fluctuations

Primary porcine aortic valve interstitial cells (pAVICs) were isolated from porcine aortic valves through a collagenase digestion process, as previously described in the literature (The relevant identification data for the primary cells have been included in the supplementary materials for reference) [24]. In this investigation, pAVICs from passages three to six were employed. The cells were cultured at 37 °C in a humidified environment with 5% CO_2, utilizing Dulbecco's Modified Eagle's Medium (DMEM; 11885-084, Gibco, Grand Island, NY, USA) supplemented with 10% fetal bovine serum (FBS; 10270-106, Gibco, Grand Island, NY, USA), 1% penicillin G and streptomycin (15140122, Gibco, Grand Island, NY, USA). The study applied a previously established method for modeling GFs *in vitro*. Upon achieving approximately 50% to 60% confluency, the cells were allocated into three distinct treatment groups: glucose control group (CTRL), high glucose (HG), and GFs. The CTRL group cells were cultured in a medium containing 5.5 mmol/L glucose, whereas the cells in the HG group were exposed to a medium with 25 mmol/L glucose. The cells in the GF group underwent alternating incubation between 5.5 mmol/L and 25 mmol/L glucose every 12 hours over a 72-hour period. Infliximab is a specific monoclonal antibody that inhibits TNF-α, exerting therapeutic effects by suppressing its proinflammatory activity. *In vitro* data obtained from ELISA in this study confirmed that infliximab treatment effectively blocks TNF-α activation (**Supplementary Fig. 2**). Concurrently, each group of pAVICs was independently exposed to 10 µg/mL of TNF-α and infliximab to examine the effects of these agents on fibrosis in pAVICs.

2.3 In Vivo Experimental Animal Models

Healthy Sprague-Dawley male rats, weighing 180–200 g, were procured from the Jiangsu Institute of Schistosomiasis Control in China. Subsequently, the rats were housed in cages equipped with food and water, situated in an environment maintained under standard conditions: temperature of 22 °C ± 2 °C, humidity levels of 55% ± 5%, and a 12-hour light–dark cycle. All experimental procedures were performed in compliance with the protocol approved by the Ethics Committee for Animal Experiments at the Affiliated Wuxi People's Hospital of Nanjing Medical University (Ethics No. DL2024015). All animal experiments conducted in this study comply with the Regulations on Laboratory Animals issued by the National Science and Technology Commission and the Implementation Rules for the Regulations on Medical Laboratory Animals promulgated by the Ministry of Health. Each cage accommodated 4–5 rats, with the bedding being routinely replaced to ensure a clean and dry environment.

To develop an animal model of diabetes in rats, we administered an intraperitoneal injection of STZ (Sigma-Aldrich Corp., St. Louis, MO, USA) at a dose of 60 mg/kg, as outlined in our previous study [9]. Rats exhibiting blood glucose levels greater than 16.7 mmol/L at one week post-injection were selected for subsequent experimental procedures. The rats were randomly allocated into five distinct groups: the glucose control group (CTRL), the persistent hyperglycemia group (HG), the diabetes with GFs group (GF), the persistent hyperglycemia with infliximab injection group (HG + IFX), and the GF with infliximab injection group (GF + IFX). In the HG + IFX and GF + IFX groups, rats received intraperitoneal injections of infliximab weekly at a dosage of 5 mg/kg for a period of eight weeks. In contrast, other groups were administered physiological saline. The CTRL group was subjected to insulin therapy, receiving long-acting insulin (glargine insulin, 20 IU/kg; Sanofi-Aventis Co., Paris, France) twice daily to ensure stable glycemic control. To induce GFs in diabetic rats, a regimen alternating between 24-hour fasting and 24-hour *ad libitum* feeding was employed [25]. During the fasting intervals, rats were administered conventional insulin (insulin Aspart, 0.5 IU/kg; Novo Nordisk Corp., Copenhagen, Denmark) to reduce blood glucose levels when they exceeded 5.5 mmol/L. Following an 8-week fasting regimen, the rats were provided with unrestricted access to food for two days, commencing 24 hours before the conclusion of the fasting period, before being euthanized for experimental purposes. For euthanasia, animals were anesthetized with 5% isoflurane, anesthesia was confirmed by tail pinch, and then sacrificed by cervical dislocation. During the experiment, aortic valves were excised, and individual samples were immediately fixed in 4% paraformaldehyde (PFA) for subsequent analysis.

2.4 Comprehensive Echocardiographic Analysis

Following the completion of the modeling process, each rat within the respective groups was marked and subsequently administered 10% pentobarbital sodium into the lower abdomen at a dosage of 50 mg/kg of the related body weight to induce anesthesia. Upon achieving adequate anesthesia, the thoracic hair of the rats was carefully removed using a hair clipper to expose the underlying

skin. Thereafter, continuous Doppler technology was employed to evaluate aortic valve function across the different rat groups, while left ventricular function was assessed using two-dimensional (2D) ultrasound technology. Specifically, the apical 3-chamber view and the parasternal long-axis view were utilized to evaluate the aortic valve and left ventricular function, respectively. For the comprehensive analysis and acquisition of essential measurement values, the built-in measurement module of the ultrasound diagnostic instrument (Philips IE33, Koninklijke Philips N.V., Amsterdam, Netherlands) was employed. The parameters for cardiac evaluation included left ventricular ejection fraction (LVEF), left ventricular fractional shortening (LVFS), left ventricular internal diameter in systole (LVIDs), left ventricular internal diameter in diastole (LVIDd), aortic root diameter, mean blood flow velocity across the aortic valve (Vmean), peak blood flow velocity across the aortic valve (Vmax), mean transvalvular pressure gradient of the aortic valve (meanPG), and peak transvalvular pressure gradient of the aortic valve (maxPG).

2.5 Histopathological Examination

The rat aortic valves were fixed in 4% PFA in phosphate-buffered saline (PBS) at 4 °C overnight. Subsequently, the tissue was dehydrated through a graded ethanol series, treated with xylene, and embedded in paraffin wax. Tissue sections, with a thickness of 6 µm, were prepared using a Leica microtome. HE staining was employed to elucidate the fundamental pathological alterations in the aortic valves of diabetic rats.

2.6 Modified Movat–Russell Pentachrome Staining

The paraffin-embedded aortic valve sections were subjected to anti-detachment treatment, followed by the application of the modified Movat–Russell pentachrome staining protocol, as recommended by the manufacturer. The stained sections were then examined microscopically, revealing distinct coloration: nuclei and elastic fibers appeared black, collagen and reticular fibers were yellow, proteoglycans exhibited a blue-green hue, cellulose-like structures and cellulose structures were dark red, and myocardial smooth muscle was red. Images were captured using a Nikon Eclipse 50i microscope (Nikon, Tokyo, Japan) in conjunction with NIS-Elements F software (NIS-Elements F software Version 4.60, Nikon, Tokyo, Japan). For the morphometric analysis of staining, a minimum of three fields per section were photographed to quantify the intensity and density of the positive signals. Image-Pro Plus 6.0 software (Image-Pro Plus software Version 6.0, Media Cybernetics, Silver Springs, MD, USA) was employed, utilizing the integrated optical density (IOD) parameter and the straw tool to identify positive signals. A selection range was established to filter out impurities, thereby ensuring the reliability of the data. The ratio of IOD to the image area (IOD/area) of the proteoglycan regions was calculated and analyzed for comparison and statistical evaluation among the different rat groups.

2.7 Immunohistochemistry

For the immunohistochemical analysis of CD3, CD68, TNF-α, collagen 1, collagen 3, α-SMA, JAK1, and STAT3 expression, our study employed transverse 4% PFA-fixed, paraffin-embedded aortic valve sections (6 µm thick). The procedure commenced with the dewaxing and hydration of the sections, followed by the inhibition of endogenous peroxidase activity using 3% hydrogen peroxide for 30 minutes. Subsequently, the sections were immersed in an EDTA antigen retrieval solution and subjected to microwave heating at high temperature for 5 minutes. This process was allowed to cool to room temperature and was repeated twice. To reduce nonspecific binding, the tissue sections were incubated with 5% goat serum at room temperature for one hour. The primary antibody was applied and incubated at 4 °C overnight. This was followed by a 60-minute incubation with a biotinylated secondary anti-rabbit and anti-mouse IgGs, and detection was performed using 3,3′-diaminobenzidine (DAB). Hematoxylin staining was applied for counterstaining. The sections were then visualized using a microscope, and the resulting images were quantitatively analyzed using Image ProPlus 6.0 software. The data are presented as the IOD/area.

2.8 Western Blot Analysis

Cells were lysed using ice-cold RIPA buffer (89900, Pierce Co., Rockford, IL, USA) supplemented with protease and phosphatase inhibitors (04693159001, Roche, Basel, Switzerland), in accordance with the manufacturer's recommended protocols. Immunoblotting was subsequently employed to analyze collagen 1, TGF-β1, p-STAT3, t-STAT3, and β-actin. The lysate was initially subjected to separation via sodium dodecyl sulfate–polyacrylamide gel electrophoresis (SDS–PAGE) and subsequently transferred onto a polyvinylidene fluoride (PVDF) membrane (10600121, Amersham Biosciences Co., Chicago, IL, USA). To prevent nonspecific binding, the PVDF membrane was then incubated with a 5% skim milk solution at room temperature for one hour. Following this blocking step, the membrane was incubated with the specified primary antibody. After the incubation period, the membrane underwent washing with PBS containing 0.05% Tween 20. Finally, the membrane was treated with a peroxidase-conjugated secondary antibody specific to the primary antibody. Following additional washing steps, the membrane was incubated with enhanced chemiluminescence reagents and subsequently exposed to X-ray film for visualization. The resulting immunoblot bands were quantified using a densitometer in conjunction with ImageJ software (Version 1.8, Scion Corp, Frederick, MD, USA). Density standardization served as a control treatment, while relative folding standardization was applied to β-actin to ensure the accuracy of the quantification process.

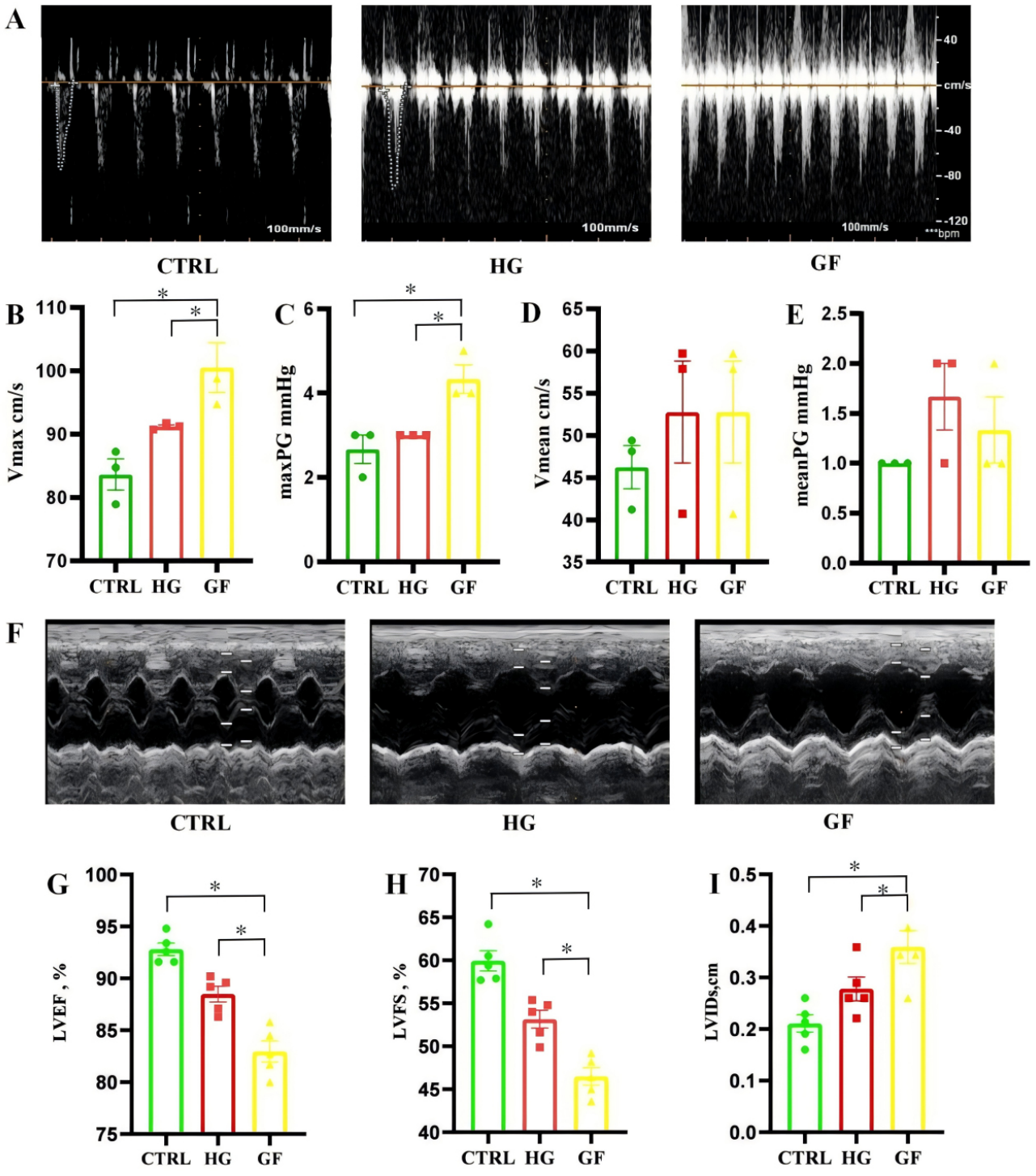

Fig. 1. Glucose fluctuations adversely affect the function of the aortic valve and left ventricular function in diabetic rat models. (A) The aortic valve functions in diabetic rats from the glucose control (CTRL), high glucose (HG), and glucose fluctuations (GF) groups. (B–E) The peak and mean blood flow velocity across the aortic valve (Vmax and Vmean), as well as the peak and mean transvalvular pressure gradients of the aortic valve (maxPG and meanPG), were measured in diabetic rats from the CTRL, HG, and GF groups (n = 3 per group). (F) The left ventricular function in three cohorts of diabetic rat models. (G–I) The left ventricular ejection fraction (LVEF), left ventricular fractional shortening (LVFS), and left ventricular internal diameter in systole (LVIDs) were assessed in diabetic rats (n = 5 per group). The data are presented as the mean ± SEM. Statistical analyses were conducted utilizing one-way ANOVA, followed by post hoc corrections to account for multiple comparisons (Fig. 1B–E, G–I). $^{*}p < 0.05$. SEM, standard error of the mean.

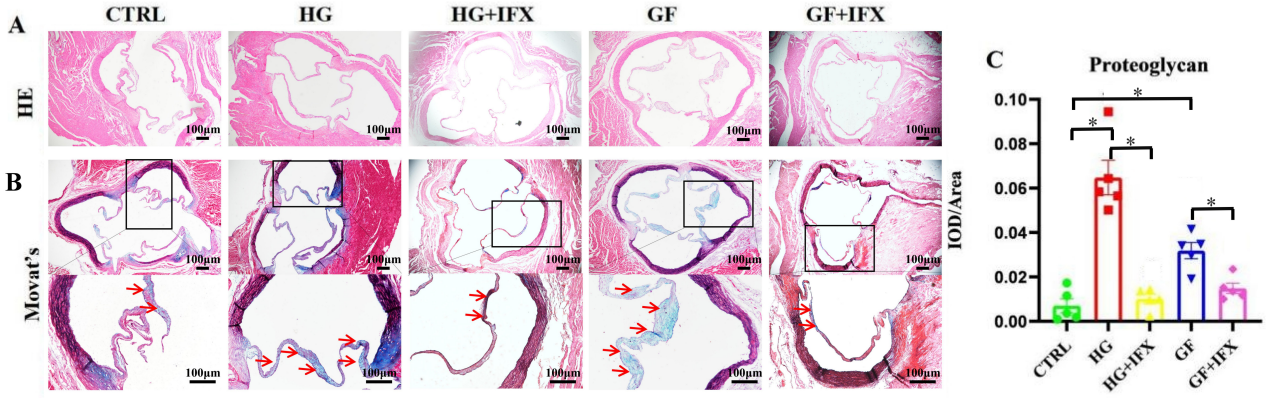

Fig. 2. Inhibition of TNF-α attenuates glucose fluctuations-induced proteoglycan deposition in the aortic valves of diabetic rat models. (A) HE staining was utilized to examine the morphology of the tricuspid aortic valves across five cohorts of diabetic rats. (B,C) Modified Movat–Russell pentachrome staining demonstrated an increased deposition of proteoglycans (indicated by arrows) in the aortic valves of the HG and GF rat cohorts in comparison to the CTRL cohort. However, administration of infliximab reduced proteoglycans (arrows) in both the HG and GF groups (n = 5 per group). The data are presented as the mean ± SEM. Statistical analyses were conducted utilizing one-way ANOVA, followed by post hoc corrections to account for multiple comparisons (Fig. 2C). $^{*}p < 0.05$, scale bar = 100 μm. TNF-α, tumor necrosis factor alpha; HE, hematoxylin and eosin; ANOVA, analysis of variance.

2.9 Immunofluorescence

To elucidate the relationship between CD3 and JAK1, as well as CD68 and JAK1 expression, immunofluorescence co-staining was conducted on the aforementioned aortic valve sections. Initially, the paraffin-embedded sections (6 μm thick) underwent dewaxing and hydration processing, followed by the inhibition of endogenous peroxidase activity using 0.3% hydrogen peroxide for 30 minutes. Subsequently, antigen retrieval was achieved by immersing the sections in an EDTA solution and subjecting them to high-temperature microwave treatment for 5 minutes. After cooling to an ambient temperature and repeating the procedure twice, the tissue slices were incubated with 5% goat serum at room temperature for one hour to reduce non-specific binding. Subsequently, primary antibodies from different species were applied and incubated at 4 °C overnight. This was followed by incubation with the corresponding fluorescent secondary antibodies at room temperature in the dark for one hour. Finally, the samples were stained with DAPI, and images were acquired from each slice using a confocal microscope. For the statistical analysis of positively stained cells by each antibody, a minimum of three fields per section were randomly selected. The intensity and density of the positive signals associated with individual cells were quantified using the Image-Pro Plus 6.0 software. The results are expressed as IOD/area.

2.10 Enzyme-Linked Immunosorbent Assay

To assess the efficacy of IFX in inhibiting TNF-α activation and its related downstream signaling pathways, specifically those involving collagen 1 and TGF-β1, we performed an ELISA on cell supernatants that had been subjected to TNF-α stimulation and IFX treatment. The preparation of samples and standards adhered strictly to the experimental protocols recommended by the manufacturer. Biotin-labeled antibodies were subsequently added, and the reaction was incubated at 37 °C for 60 minutes. Following this, the samples underwent three washes with PBS, after which an avidin–biotin complex (ABC) was introduced, and the reaction was maintained at 37 °C for an additional 30 minutes. The samples were then washed five times with PBS before the addition of the tetramethylbenzidine (TMB) substrate, allowing the reaction to proceed at 37 °C for 15 to 20 minutes. A stop solution was subsequently applied, and the optical density (OD) was measured using a plate reader. A standard curve was generated from the standards to quantify the concentration of the samples.

2.11 Statistical Analysis

Data are presented as the mean ± standard error of the mean (SEM). Statistical analyses were conducted using IBM SPSS Statistics Version 2.0 software (IBM, Armonk, NY, USA). For comparisons between two groups, Gaussian-distributed numerical variables were analyzed using the Student's *t*-test, preceded by Levene's test for equality of variance. For comparisons involving three or more groups, a one-way analysis of variance (ANOVA) was utilized, with subsequent pairwise comparisons performed using Tukey's honestly significant difference (HSD) test. Non-Gaussian numerical variables were evaluated using the Mann–Whitney non-parametric test. Two-sided probability *p*-values < 0.05 were considered statistically significant.

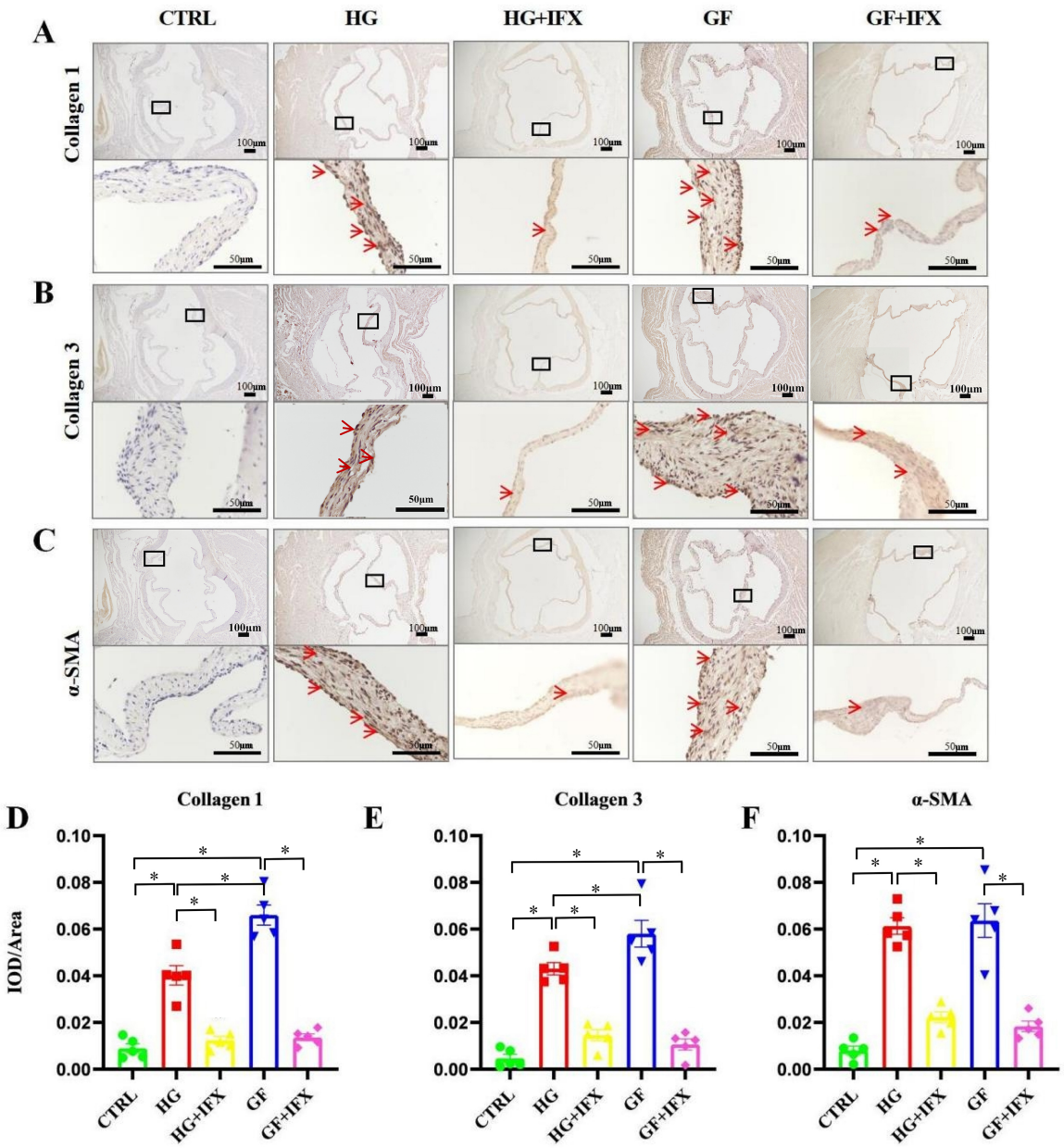

Fig. 3. Inhibition of TNF-α mitigates glucose fluctuations-induced aortic valve fibrosis. (A,B,D,E) Immunohistochemical staining for collagen 1 and 3 (indicated by arrows) demonstrated enhanced collagen deposition in the aortic valves of the HG and GF diabetic rat models. However, treatment with infliximab was observed to mitigate this collagen accumulation. (C,F) Immunohistochemical analysis for α-SMA (arrows) revealed an increased fibrotic response in the aortic valves of the diabetic rats in the HG and GF groups; however, infliximab treatment reduced this progression (n = 5 per group). The data are presented as the mean $\pm$ SEM. Statistical analyses were conducted utilizing one-way ANOVA, followed by post hoc corrections to account for multiple comparisons (Fig. 3D–F). $^{*}p < 0.05$, scale bar = 50 µm or 100 µm. α-SMA, α-smooth muscle actin.

3. Results

3.1 Glucose Fluctuations Impair the Function of the Aortic Valve and Left Ventricle in Diabetic Rats

As depicted above, three distinct groups of rat models were established to examine the effects of GFs on aortic valve function in diabetic rats: CTRL, HG, and GF. The cardiac ultrasound results for these groups after 8 weeks are presented in Fig. 1 (Fig. 1A,F). Compared to both the CTRL and HG groups, the GF group demonstrated significantly elevated Vmax and maxPG values, with these differences reaching statistical significance ($p < 0.05$). Although the Vmax and maxPG values in the HG group were higher than those in the CTRL group, the difference did not attain

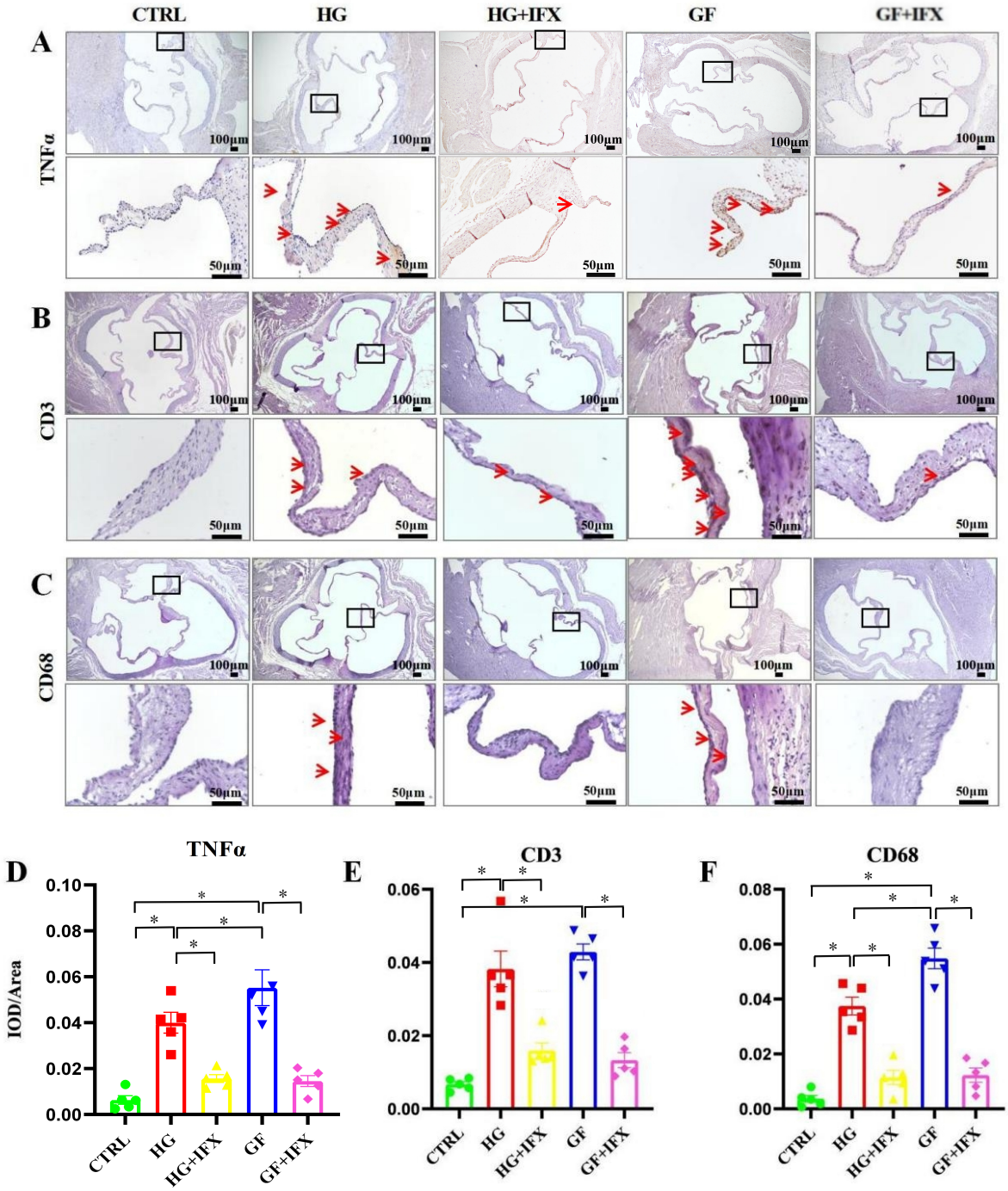

Fig. 4. Inhibition of TNF-α reduced inflammation induced by glucose fluctuations in the aortic valves of diabetic rat models. (A,D) Immunostaining for TNF-α (indicated by arrows) revealed an elevated expression of the TNF-α protein in the aortic valves of the HG group, with an even greater upregulation observed in the GF group. Notably, the inhibition of TNF-α effectively reversed this upregulation in both the HG and GF groups. (B,E) The HG and GF groups exhibited an increased infiltration of CD3-positive T lymphocytes compared to the CTRL group; however, this increase could be mitigated by the inhibition of TNF-α. (C,F) The HG group showed increased CD68-positive macrophage infiltration compared to the CTRL group, and the GF group showed even higher levels; however, TNF-α inhibition could reduce this upregulation (n = 5 per group). The data are presented as the mean $\pm$ SEM. Statistical analyses were conducted utilizing one-way ANOVA, followed by post hoc corrections to account for multiple comparisons (Fig. 4D–F). $^{*}p < 0.05$, scale bar = 50 μm or 100 μm.

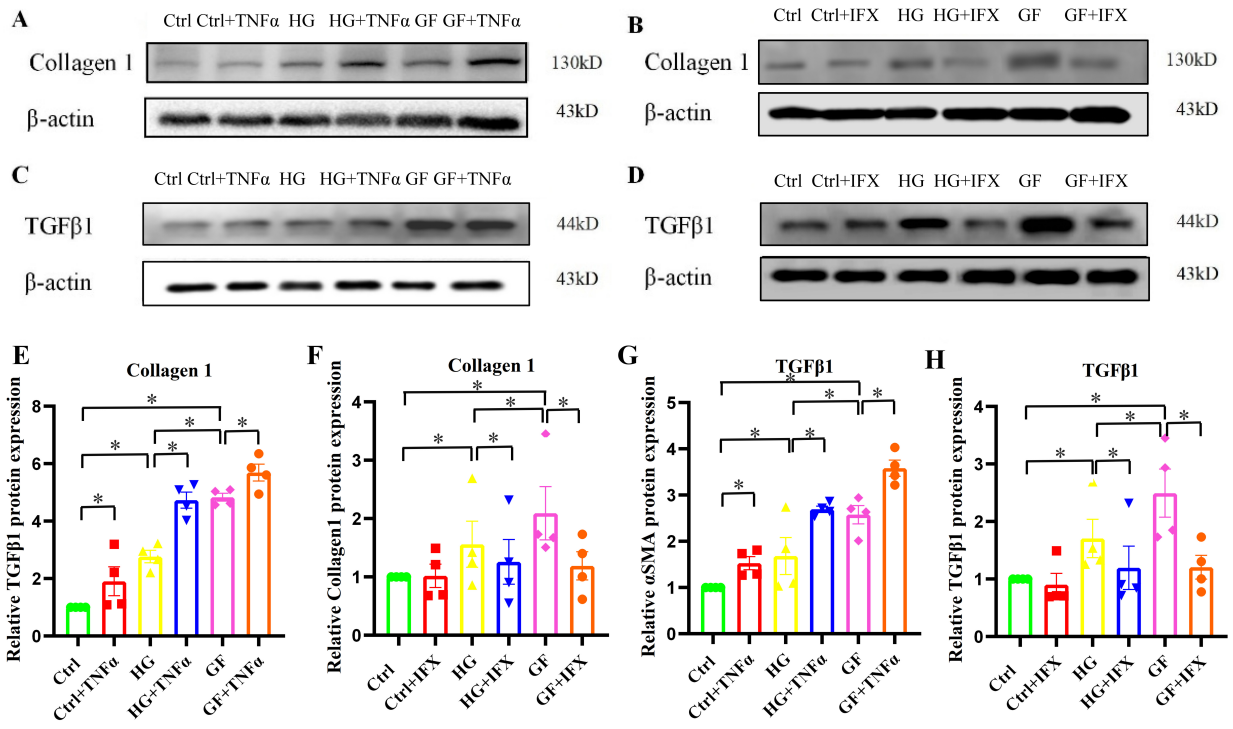

Fig. 5. TNF-α-mediated inflammation could exacerbate fibrosis *in vitro* in porcine aortic valve interstitial cells across different glucose levels. (A,B,E,F) In the primary porcine aortic valve interstitial cells (pAVICs) groups, both HG and GF conditions were found to upregulate collagen 1 protein expression. Moreover, the proinflammatory cytokine TNF-α aggravated this upregulation under HG conditions, with an even more pronounced effect observed under GF conditions. Conversely, the inhibition of TNF-α could reverse these upregulations in both the HG and GF groups. (C,D,G,H) TGF-β1 protein expression increased under both HG and GF conditions, with TNF-α further enhancing this increase, especially under GF conditions. The inhibition of TNF-α reversed these effects in both groups (n = 4 per group). The data are presented as the mean $\pm$ SEM. Statistical analyses were conducted utilizing one-way ANOVA, followed by post hoc corrections to account for multiple comparisons (Fig. 5E–H). $^{*}p < 0.05$.

statistical significance (Fig. 1B,C). Meanwhile, there were no significant differences in the Vmean and meanPG values among the three groups of rats (Fig. 1D,E). Similarly, the inner diameter of the aortic root did not differ significantly among the groups. However, further examination of the impact of blood glucose concentration on left ventricular function revealed that the GF group exhibited significantly reduced LVEF and LVFS compared to the HG group, with these reductions being more pronounced than those observed in the CRTL group (Fig. 1G,H). Furthermore, the LVIDs in the GF group of rats were markedly increased in comparison to both the HG and CTRL groups. Importantly, there was no statistically significant difference in the LVIDd among the three groups (Fig. 1I).

3.2 Glucose Fluctuations Exacerbate Aortic Valve Fibrosis in Diabetic Rats

The rat aortic valve sections underwent HE staining as well as modified Movat–Russell pentachrome staining to assess the effects of GFs on aortic valve function *in vivo*. The findings demonstrated heightened expression of proteoglycans in the aortic valve specimens from the HG and GF groups compared to the CTRL group. Furthermore, the aortic valve in the GF group displayed increased thickening relative to the HG group, although the expression level of proteoglycans was not significantly increased (Fig. 2A–C). Immunohistochemical analysis indicated a significant upregulation in collagen 1, collagen 3, and α-SMA expression in the rat aortic valve samples from the HG and GF groups compared to the CTRL group (Fig. 3A–C). Notably, the expressions of collagen 1 and collagen 3 were significantly elevated in the GF group relative to the HG group, whereas the α-SMA levels did not exhibit significant variations (Fig. 3D–F). These results collectively indicate an enhancement in the fibrotic morphology of the aortic valve in diabetic rats subjected to fluctuations in glucose levels.

3.3 Glucose Fluctuations Result in Enhanced Infiltration of TNF-α In Vivo, Accompanied by Elevated CD3 and CD68 Expressions

Immunohistochemical analysis of the rat aortic valves was employed to quantify the expression levels of inflam-

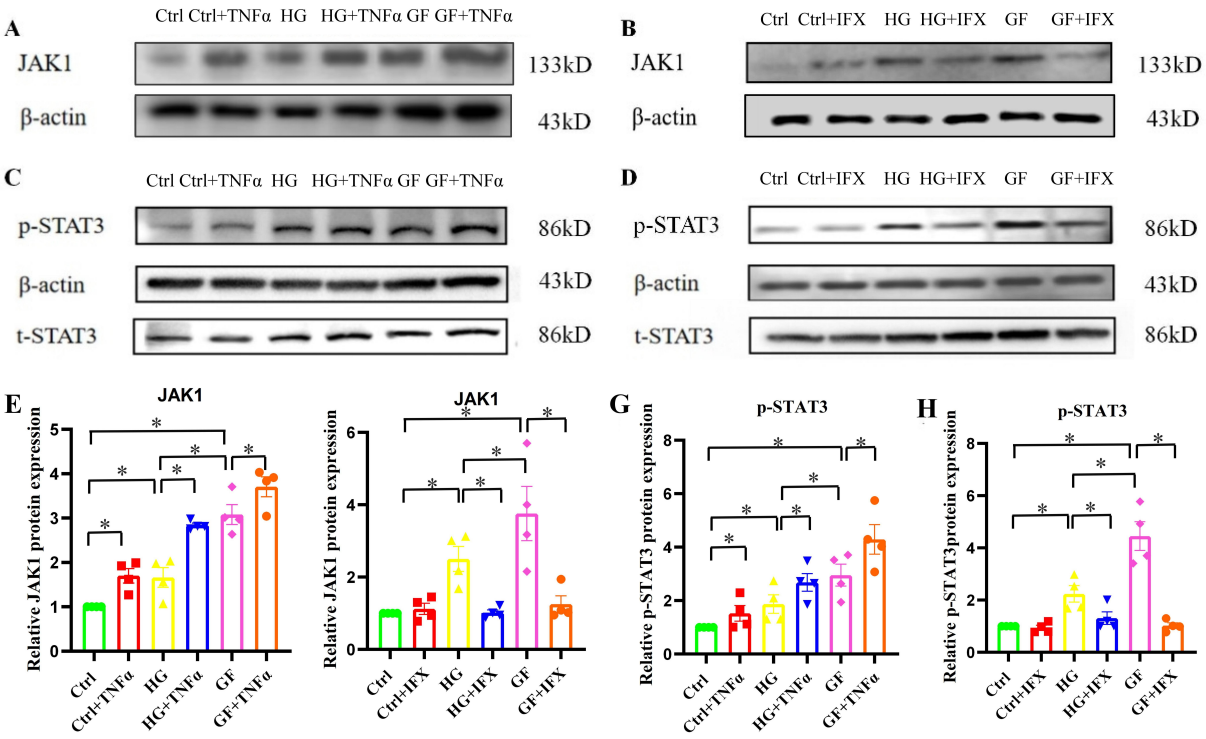

Fig. 6. TNF-α activated the JAK1/STAT3 pathway *in vitro* in porcine aortic valve interstitial cells under varying glucose concentrations. (A,B,E,F) In the pAVIC groups, both the HG and GF conditions upregulated the JAK1 protein expression. The presence of TNF-α exacerbated this upregulation under HG conditions, with a more pronounced effect observed under GF conditions. Conversely, the inhibition of TNF-α effectively reversed these upregulations in both the HG and GF groups. (C,D,G,H) In the pAVIC groups, phospho-STAT3 protein expression increased under both the HG and GF conditions, with TNF-α further enhancing this increase, especially in the GF conditions. Inhibiting TNF-α reversed these effects in both the HG and GF groups (n = 4 per group). The data are presented as the mean $\pm$ SEM. Statistical analyses were conducted utilizing one-way ANOVA, followed by post hoc corrections to account for multiple comparisons (Fig. 6E–H). $^{*}p < 0.05$. JAK1, Janus kinase 1; STAT3, signal transducer and activator of transcription 3.

matory markers CD3, CD68, and TNF-α. Our results indicated a significant upregulation of these markers in both the GF and HG groups compared to the CTRL group (Fig. 4A–C). Importantly, the expression levels of CD68 and TNF-α were markedly higher in the GF group relative to the HG group (Fig. 4D,F). Interestingly, a substantial reduction in the expression of these inflammatory markers was observed after intraperitoneal administration of infliximab (Fig. 4D–F).

3.4 Elevated Infiltration of TNF-α Facilitates Diabetes Associated Aortic Valve Fibrosis and Inhibition of TNF-α May Mitigate This Fibrotic Process

In this study, the expression of fibrosis-associated proteins in pAVICs was evaluated *in vitro* using Western blot analysis across three groups: CTRL, HG, and GF. The findings indicated that the GF group exhibited elevated levels of TGF-β1 and collagen 1 compared to the HG group, which, in turn, showed higher levels than the CTRL group. Furthermore, treatment with the TNF-α protein at a concentration of 10 µg/mL resulted in a significant upregulation of TGF-β1 and collagen 1 expression in all three groups (Fig. 5A,C,E,G). There was a significant reduction in the expression levels of TGF-β1 and collagen 1 in both the HG and GF groups upon administration of infliximab at a concentration of 10 µg/mL (Fig. 5B,D,F,H). These findings were corroborated by an immunohistochemical analysis, which demonstrated that intraperitoneal administration of infliximab reduced the expression of the fibrotic proteins TGF-β1 and collagen 1 within the valve tissue of rats in the HG + IFX and GF + IFX groups, compared to the HG and GF groups (Fig. 3A–F).

3.5 JAK1/STAT3 Signaling Pathway Regulation in Aortic Valve Fibrosis is Associated With TNF-α-Mediated Glucose Fluctuations

In further *in vitro* experiments incorporating Western Blot analysis, the expression levels of JAK1 and STAT3 protein were elevated in the GF and HG groups relative to the CTRL group, with the GF group exhibiting the most

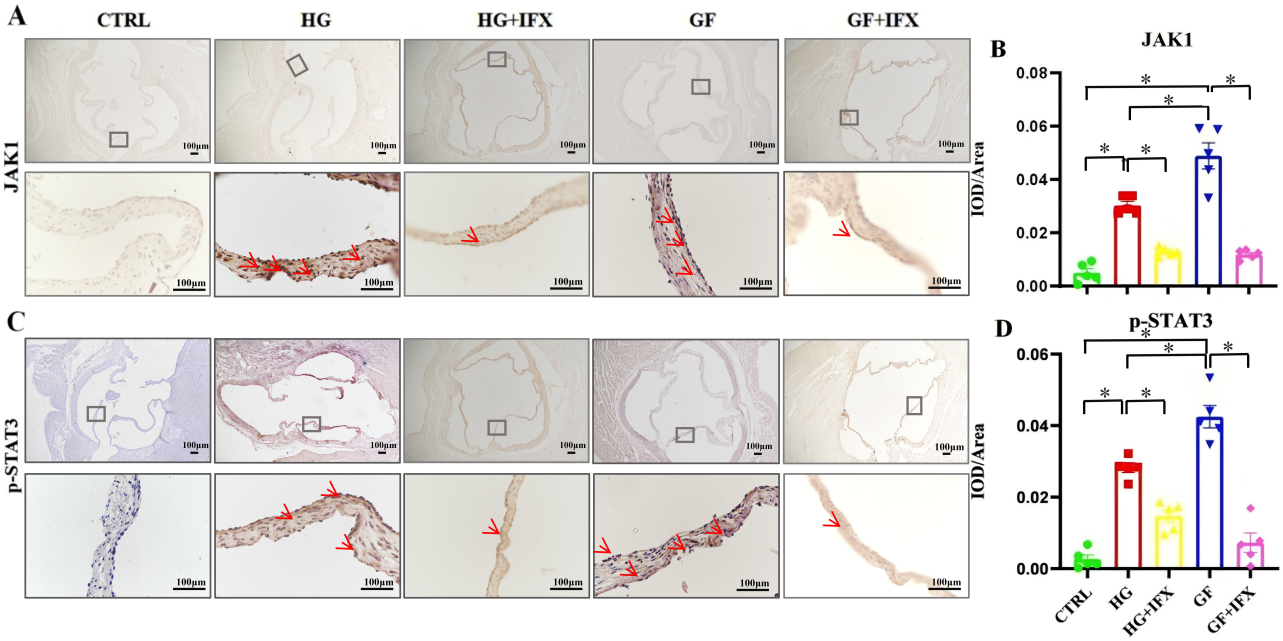

Fig. 7. Inhibition of TNF-α led to the downregulation of the JAK1/STAT3 pathway *in vivo* in the aortic valves of diabetic rat models. (A,B) Immunohistochemical analysis of JAK1 (indicated by arrows) revealed an upregulation in JAK1 protein expression in the aortic valves of both HG and GF diabetic rat models. Notably, administration of infliximab was found to attenuate this upregulation. (C,D) Immunohistochemistry showed increased p-STAT3 protein expression in the aortic valves of the HG and GF diabetic rats, which was attenuated by the inhibition of TNF-α treatment. n = 5 per group. The data are presented as the mean $\pm$ SEM. Statistical analyses were conducted utilizing one-way ANOVA, followed by post hoc corrections to account for multiple comparisons (Fig. 7B,D). $^{*}p < 0.05$, scale bar = 100 μm.

pronounced upregulation. The application of the TNF-α protein at a concentration of 10 μg/mL further augmented the expression of JAK1 and STAT3 in pVICs within the CTRL + TNF-α, HG + TNF-α, and GF + TNF-α groups compared to their respective CTRL, HG, and GF counterparts (Fig. 6A,C,E,G). Subsequently, treatment with 10 μg/mL infliximab resulted in a significant reduction in the expression levels of JAK1 and STAT3 (Fig. 6B,D,F,H). Immunohistochemical analysis of the JAK1 and STAT3 protein expressions in the aortic valves of five rat cohorts revealed that the HG and GF groups exhibited significantly elevated expression levels compared to the CTRL group, with the GF group demonstrating the highest expression. Moreover, administration of infliximab via intraperitoneal injection reduced the JAK1 and STAT3 expressions in both the HG + IFX and GF + IFX groups (Fig. 7A–D).

3.6 The Interaction Between JAK1 and T Cells, as Well as Macrophages

Utilizing immunofluorescence co-staining techniques, this study investigated the spatial and quantitative associations between JAK1 and CD3, as well as JAK1 and CD68. This analysis revealed an enhancement in the co-localization of JAK1 with CD3 and CD68 in both the GF and HG experimental groups (Fig. 8). Notably, the GF group exhibited a greater increase compared to the HG group. Meanwhile, a reduction in the co-staining of JAK1, CD3, and CD68 was observed after infliximab administration via intraperitoneal injection (Fig. 8A,B).

4. Discussion

GFs exert more detrimental effects than persistent hyperglycemia in the development and progression of cardiovascular complications associated with diabetes; however, the underlying mechanisms remain inadequately understood [26–29]. This study represents the first investigation into the molecular mechanisms through which blood GFs influence AVF within the framework of diabetic cardiovascular complications. Notably, our findings indicate that GFs have a more pronounced impact on AVF than sustained hyperglycemia, with GFs exacerbating AVF more significantly than sustained hyperglycemia, a phenomenon associated with elevated expression levels of collagen 1. Furthermore, our study highlights the critical role of TNF-α in the pathogenesis of glucose-induced AVF. Additionally, we discovered that GFs activate the JAK1/STAT3 signaling pathway, resulting in the upregulation of downstream proteins related to fibrosis.

In comparison to non-diabetic individuals, patients with diabetes are more prone to metabolic abnormalities

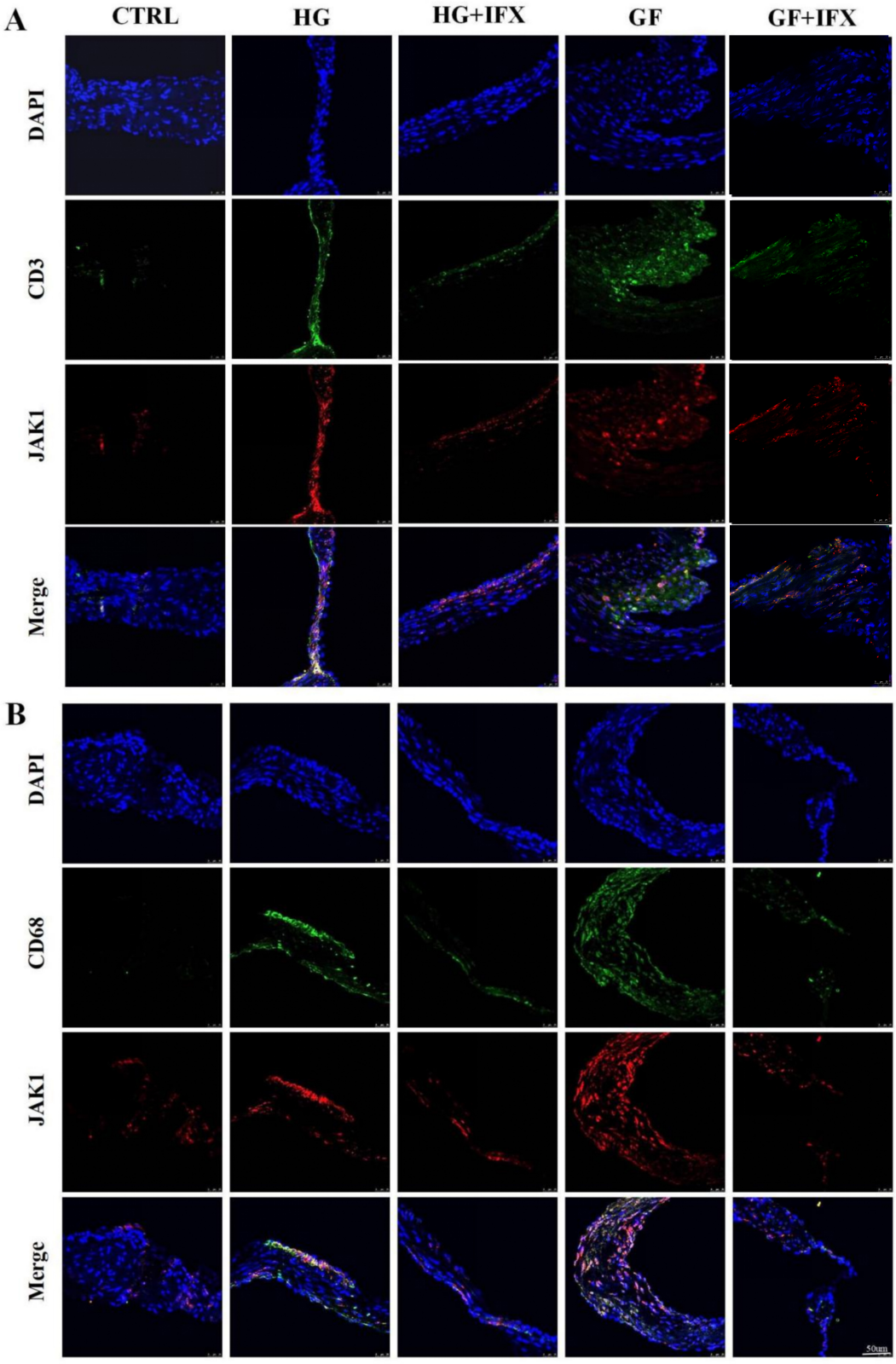

Fig. 8. Colocalization of CD3, CD68, and JAK1 in the aortic valves of diabetic rat models. (A,B) The coimmunostaining analysis of the HG and GF groups demonstrated the presence of CD3, CD68, and JAK1 proteins, indicating that JAK1 expression is primarily localized in T lymphocytes and macrophages. Notably, this expression pattern could be altered through the inhibition of TNF-α. Scale bar = 50 µm. DAPI, 4′,6-diamidino-2-phenylindole.

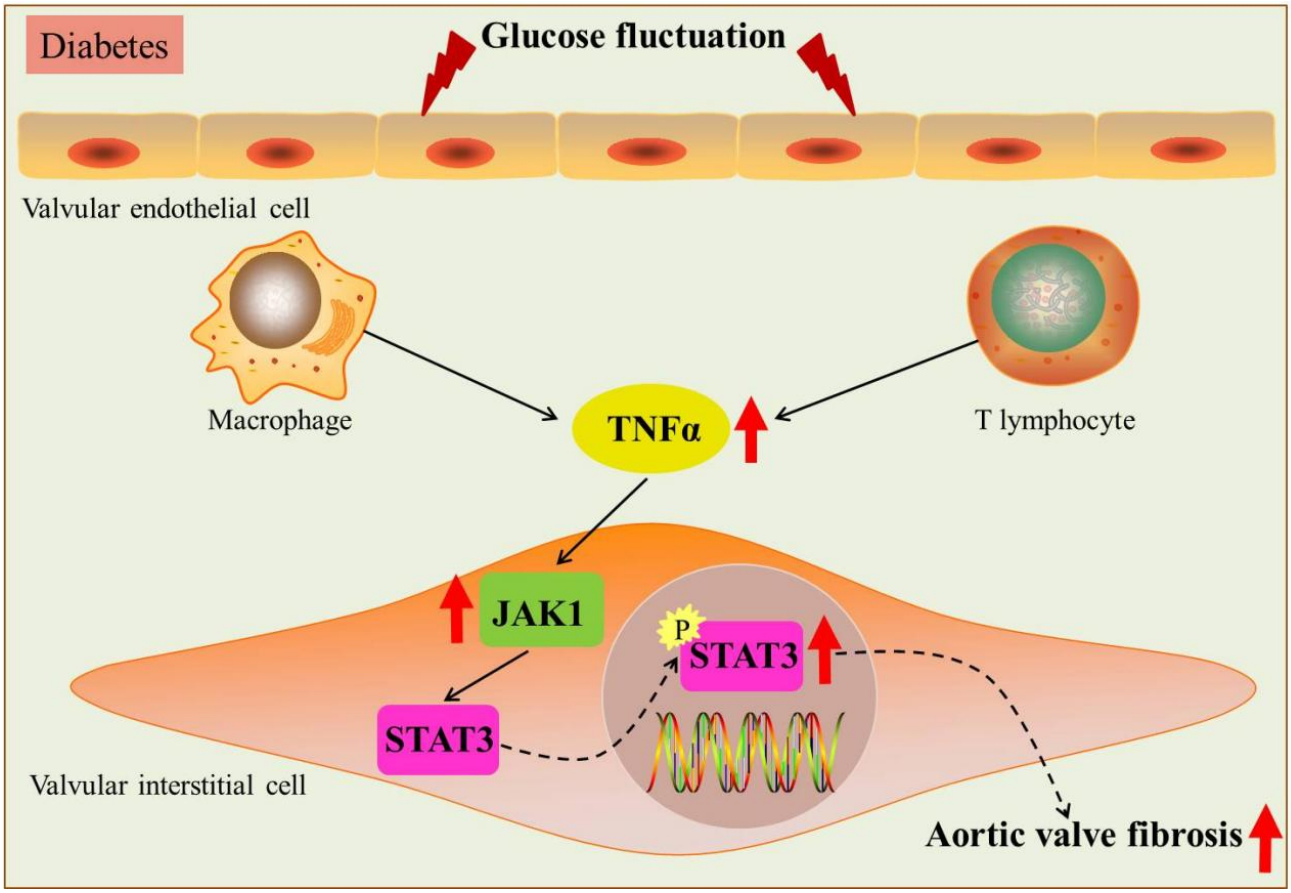

Fig. 9. A working model of TNF-α-mediated JAK1/STAT3 pathway activation in glucose fluctuation-induced aortic valve fibrosis. GFs induce damage to VECs, which subsequently enhances the infiltration of macrophages and T lymphocytes, along with the secretion of TNF-α, and the activation of VICs. This cascade further augments the inflammatory signaling pathway, particularly through the upregulation of JAK1/STAT3. The phosphorylation of STAT3 facilitates its translocation into the nucleus, where it promotes the upregulation of fibrotic factors, thereby exacerbating the AVF. Red arrows: the specific proteins up-regulated.

that can lead to structural and functional changes in the aortic valves [30,31]. Notably, diabetic patients with aortic valve disease exhibit heightened levels of calcification, experience accelerated disease progression, and frequently encounter a poorer prognosis [32,33]. AVF, regarded as a preclinical stage of CAVD, may represent a pivotal point for early therapeutic intervention. Early therapeutic interventions at the initial stage of AVF may impede or slow the progression of CAVD. Therefore, it is crucial to investigate the specific mechanisms through which diabetes induces AVF. This research holds promise for the development of new strategies to prevent and manage this condition. Therefore, this study establishes diabetic rat models with controlled, uncontrolled, and fluctuating blood glucose levels to assess the impact of blood glucose levels on valve fibrosis. In the experiment, the diabetes group with controlled blood glucose serves as the control group, based on the baseline data, to evaluate the condition of AVF. However, due to the absence of a non-diabetic wild-type control group, certain limitations remained when assessing the effect of blood GFs on AVF.

Recent findings have demonstrated that CAVD arises from complex and dynamic cellular mechanisms involving VICs, VECs, and inflammatory cells, which collectively contribute to the remodeling of the extracellular matrix (ECM) [34–36]. Furthermore, collagen 1 and collagen 3 are predominantly expressed as ECM proteins within the aortic valve [37,38]. Our study indicates that the aortas of diabetic rats experiencing fluctuating blood glucose levels exhibit significant fibrosis, accompanied by an upregulation in the expression of collagen 1. In addition, the results of the modified Movat–Russell pentachrome staining demonstrated an increase in proteoglycans within the aortic valves of diabetic rats experiencing fluctuating blood glucose levels. Our research findings suggest that GFs exert a more detrimental effect on aortic valve function than sustained hyperglycemia. Moreover, in comparison to persistent hyperglycemia, GFs more significantly exacerbate AVF by upregulating the expression of collagen 1 to a greater extent. Nonetheless, the expression of α-SMA did not exhibit a significant increase compared to the HG group, potentially due to the activation of distinct pathways involved

in valvular fibrosis. Collagen, a crucial component of the ECM, undergoes excessive deposition, which is a hallmark of fibrosis. The expression of collagen 1 is typically regulated by signaling pathways such as TGF-β and connective tissue growth factor (CTGF). Meanwhile, α-SMA serves as a marker of myofibroblasts, while the upregulation of α-SMA is closely associated with the progression of fibrosis. Indeed, the expression of α-SMA increases during the differentiation of VICs into fibroblasts. Therefore, we hypothesized that GFs enhance collagen deposition primarily by increasing the activation of the TGF-β pathway, rather than promoting the differentiation of interstitial cells into fibroblasts. This hypothesis requires further experimental validation.

Research has demonstrated that individuals with diabetes experience chronic systemic inflammation [39,40]. Previous studies have shown that diabetes can cause specific molecular changes in valve endothelial cells, promote monocyte infiltration, and contribute to endothelial dysfunction [41]. During infiltration, inflammatory cells release significant quantities of TNF-α, which influences various aspects of aortic valve calcification, including exacerbating VEC injury, enhancing monocyte adhesion, and facilitating the formation of foam cells [42,43]. Our research results indicate that during GFs, the infiltration of inflammatory cells in the aortic valve increases, and a large number of inflammatory factors are secreted, mainly manifested as an upregulation in TNF-α expression. However, in addition to the presence of inflammatory infiltrating cells, it is plausible that VICs may produce TNF-α in response to stimulation or an enhanced reaction to GFs. This hypothesis requires further empirical validation.

Chronic inflammation plays a crucial role in the progression of CAVD [44–46]. However, the exact mechanism involved remains unclear, while an effective target also needs to be identified to alleviate this process. To our knowledge, this study is the first to elucidate the molecular mechanism through which GFs affect AVF within the context of cardiovascular complications in diabetes. This study aimed to investigate the impact of TNF-α on glucose-induced AVF, with a particular focus on the activation of downstream signaling pathways resulting from increased infiltration of inflammatory cells. In particular, the research focused on the JAK1/STAT3 signaling pathway, a crucial mediator of the inflammatory response. We utilized echocardiography to assess aortic valve and left ventricular function in rats with high glucose levels and GFs. Subsequently, we implemented the TNF-α inhibitor, infliximab, as an intervention strategy. Further validation of aortic valve and left ventricular function in the HG + IFX and GF + IFX rat groups could provide a more comprehensive understanding of the specific effects of TNF-α on these structures. After intraperitoneal injection of infliximab into glucose fluctuating rats, inflammation infiltration in the valves decreased *in vivo*, and valve fibrosis also improved. Moreover, a significant decrease was observed in the expression levels of critical proteins associated with fibrosis, including JAK1, STAT3, collagen 1, and TGF-β1, following the application of infliximab to cultured rat aortic valves. These findings indicate that targeting TNF-α may effectively modulate the inflammatory response and attenuate the progression of glucose-induced AVF, underscoring the critical role of inflammatory pathways in this pathological process. This study provides evidence to support the potential of inhibiting the TNF-α/JAK1/STAT3 pathway in preventing the progression of valve calcification. Further clinical studies are needed to investigate the safety and efficacy of this treatment in CAVD.

5. Conclusions

This study suggests that, in comparison to persistent hyperglycemia, GFs lead to impaired endothelial cell function, increased infiltration of inflammatory cells, and elevated secretion of TNF-α, which acts on AVICs. This process enhances the expression of the JAK1/STAT3 signaling pathway, thereby exacerbating the expression of fibrosis-related proteins and facilitating the development and progression of AVF (Fig. 9). These findings suggest that GFs may constitute a more significant risk factor of AVF than persistent hyperglycemia. Consequently, improved management of GFs could emerge as a novel therapeutic strategy in clinical practice, potentially aiding in the deceleration and reversal of AVF in individuals with diabetes.

Availability of Data and Materials

All data generated or analyzed during this study are included in this article and its **Supplementary material files**. Further enquiries can be directed to the corresponding author.

Author Contributions

Study concept and design: FX, RXW, KLL and YJC. Acquisition, analysis, or interpretation of data: YJC, HPC, CYZ and XSR. Drafting of the manuscript: YJC and FX. Critical revision of the manuscript for important intellectual content: All authors. Obtained funding: FX and RXW. Administrative, technical, or material support: CYZ, XSR, KLL, FX and RXW. YJC, HPC, FX and RXW had full access to all the data in the study and took responsibility for the integrity of the data and the accuracy of the data analysis. All authors read and approved the final manuscript. All authors contributed to editorial changes in the manuscript. All authors have participated sufficiently in the work and agreed to be accountable for all aspects of the work.

Ethics Approval and Consent to Participate

All experimental procedures were performed in compliance with the protocol approved by the Ethics Committee for Animal Experiments at the Affiliated Wuxi Peo-

ple's Hospital of Nanjing Medical University (Ethics No. DL2024015). All animal experiments conducted in this study comply with the Regulations on Laboratory Animals issued by the National Science and Technology Commission and the Implementation Rules for the Regulations on Medical Laboratory Animals promulgated by the Ministry of Health.

Acknowledgment

Thanks to all the peer reviewers for their opinions and suggestions.

Funding

This study was supported by the National Natural Science Foundation of China (No. 81800340, No. 82370342), Natural Science Foundation of Jiangsu Province (No. BK20231145), Top Talent Support Program for Young and Middle-Aged People of Wuxi Health Committee (No. HB2023007), and Wuxi Medical Center, Nanjing Medical University (WMCG202514).

Conflict of Interest

The authors declare no conflict of interest.

Supplementary Material

Supplementary material associated with this article can be found, in the online version, at https://doi.org/10.31083/RCM42804.

References

[1] Kraler S, Blaser MC, Aikawa E, Camici GG, Lüscher TF. Calcific aortic valve disease: from molecular and cellular mechanisms to medical therapy. European Heart Journal. 2022; 43: 683–697. https://doi.org/10.1093/eurheartj/ehab757.

[2] Fan L, Yao D, Fan Z, Zhang T, Shen Q, Tong F, *et al*. Beyond VICs: Shedding light on the overlooked VECs in calcific aortic valve disease. Biomedicine & Pharmacotherapy = Biomedecine & Pharmacotherapie. 2024; 178: 117143. https://doi.org/10.1016/j.biopha.2024.117143.

[3] Moncla LHM, Briend M, Bossé Y, Mathieu P. Calcific aortic valve disease: mechanisms, prevention and treatment. Nature Reviews. Cardiology. 2023; 20: 546–559. https://doi.org/10.1038/s41569-023-00845-7.

[4] Chen Y, Xiao F, Wang R. Calcified aortic valve disease complicated with and without diabetes mellitus: the underlying pathogenesis. Reviews in Cardiovascular Medicine. 2022; 23: 7. https://doi.org/10.31083/j.rcm2301007.

[5] Choi B, Kim EY, Kim JE, Oh S, Park SO, Kim SM, *et al*. Evogliptin Suppresses Calcific Aortic Valve Disease by Attenuating Inflammation, Fibrosis, and Calcification. Cells. 2021; 10: 57. https://doi.org/10.3390/cells10010057.

[6] Raddatz MA, Madhur MS, Merryman WD. Adaptive immune cells in calcific aortic valve disease. American Journal of Physiology. Heart and Circulatory Physiology. 2019; 317: H141–H155. https://doi.org/10.1152/ajpheart.00100.2019.

[7] Lu Y, Wang W, Liu J, Xie M, Liu Q, Li S. Vascular complications of diabetes: A narrative review. Medicine. 2023; 102: e35285. https://doi.org/10.1097/MD.0000000000035285.

[8] Corbacho-Alonso N, Sastre-Oliva T, López-Almodovar LF, Sotlis J, Padial LR, Tejerina T, *et al*. Diabetes mellitus and aortic stenosis head to head: toward personalized medicine in patients with both pathologies. Translational Research: the Journal of Laboratory and Clinical Medicine. 2023; 259: 35–45. https://doi.org/10.1016/j.trsl.2023.04.002.

[9] Zhang ZY, Qian LL, Wang N, Miao LF, Ma X, Dang SP, *et al*. Glucose fluctuations promote vascular BK channels dysfunction via PKCα/NF-κB/MuRF1 signaling. Journal of Molecular and Cellular Cardiology. 2020; 145: 14–24. https://doi.org/10.1016/j.yjmcc.2020.05.021.

[10] Zhang L, Liu HH, Yang F, Zhang ZY, Zhang ZY, Zhao XX, *et al*. Glucose fluctuations aggravate myocardial fibrosis via activating the CaMKII/Stat3 signaling in type 2 diabtetes. Diabetology & Metabolic Syndrome. 2023; 15: 217. https://doi.org/10.1186/s13098-023-01197-5.

[11] Xue Y, Zeng X, Tu WJ, Zhao J. Tumor Necrosis Factor-α: The Next Marker of Stroke. Disease Markers. 2022; 2022: 2395269. https://doi.org/10.1155/2022/2395269.

[12] Aggarwal BB. Tumour necrosis factors receptor associated signalling molecules and their role in activation of apoptosis, JNK and NF-kappaB. Annals of the Rheumatic Diseases. 2000; 59 Suppl 1: i6–16. https://doi.org/10.1136/ard.59.suppl_1.i6.

[13] Mathieu P, Bouchareb R, Boulanger MC. Innate and Adaptive Immunity in Calcific Aortic Valve Disease. Journal of Immunology Research. 2015; 2015: 851945. https://doi.org/10.1155/2015/851945.

[14] Xu K, Huang Y, Zhou T, Wang C, Chi Q, Shi J, *et al*. Nobiletin exhibits potent inhibition on tumor necrosis factor alpha-induced calcification of human aortic valve interstitial cells via targeting ABCG2 and AKR1B1. Phytotherapy Research: PTR. 2019; 33: 1717–1725. https://doi.org/10.1002/ptr.6360.

[15] Yu Z, Seya K, Daitoku K, Motomura S, Fukuda I, Furukawa KI. Tumor necrosis factor-α accelerates the calcification of human aortic valve interstitial cells obtained from patients with calcific aortic valve stenosis via the BMP2-Dlx5 pathway. The Journal of Pharmacology and Experimental Therapeutics. 2011; 337: 16–23. https://doi.org/10.1124/jpet.110.177915.

[16] Parra-Izquierdo I, Sánchez-Bayuela T, López J, Gómez C, Pérez-Riesgo E, San Román JA, *et al*. Interferons Are Pro-Inflammatory Cytokines in Sheared-Stressed Human Aortic Valve Endothelial Cells. International Journal of Molecular Sciences. 2021; 22: 10605. https://doi.org/10.3390/ijms221910605.

[17] Liu X, Zheng Q, Wang K, Luo J, Wang Z, Li H, *et al*. Sam68 promotes osteogenic differentiation of aortic valvular interstitial cells by TNF-α/STAT3/autophagy axis. Journal of Cell Communication and Signaling. 2023; 17: 863–879. https://doi.org/10.1007/s12079-023-00733-2.

[18] Hu X, Li J, Fu M, Zhao X, Wang W. The JAK/STAT signaling pathway: from bench to clinic. Signal Transduction and Targeted Therapy. 2021; 6: 402. https://doi.org/10.1038/s41392-021-00791-1.

[19] Tanaka Y, Luo Y, O'Shea JJ, Nakayamada S. Janus kinase-targeting therapies in rheumatology: a mechanisms-based approach. Nature Reviews. Rheumatology. 2022; 18: 133–145. https://doi.org/10.1038/s41584-021-00726-8.

[20] Philips RL, Wang Y, Cheon H, Kanno Y, Gadina M, Sartorelli V, *et al*. The JAK-STAT pathway at 30: Much learned, much more to do. Cell. 2022; 185: 3857–3876. https://doi.org/10.1016/j.cell.2022.09.023.

[21] Hao N, Zhou Z, Zhang F, Li Y, Hu R, Zou J, *et al*. Interleukin-29 Accelerates Vascular Calcification via JAK2/STAT3/BMP2 Signaling. Journal of the American Heart Association. 2023; 12: e027222. https://doi.org/10.1161/JAHA.122.027222.

[22] Baldini C, Moriconi FR, Galimberti S, Libby P, De Caterina R. The JAK-STAT pathway: an emerging target for cardiovascu-

lar disease in rheumatoid arthritis and myeloproliferative neoplasms. European Heart Journal. 2021; 42: 4389–4400. https://doi.org/10.1093/eurheartj/ehab447.

[23] Parra-Izquierdo I, Sánchez-Bayuela T, Castaños-Mollor I, López J, Gómez C, San Román JA, *et al*. Clinically used JAK inhibitor blunts dsRNA-induced inflammation and calcification in aortic valve interstitial cells. The FEBS Journal. 2021; 288: 6528–6542. https://doi.org/10.1111/febs.16026.

[24] Xiao F, Pan H, Yang D, Wang R, Wu B, Shao Y, *et al*. Identification of TNFα-mediated inflammation as potential pathological marker and therapeutic target for calcification progress of congenital bicuspid aortic valve. European Journal of Pharmacology. 2023; 951: 175783. https://doi.org/10.1016/j.ejphar.2023.175783.

[25] Zhang ZY, Pan L, Dang S, Wang N, Zhao SY, Li F, *et al*. Glucose fluctuations aggravate cardiomyocyte apoptosis by enhancing the interaction between Txnip and Akt. BMC Cardiovascular Disorders. 2024; 24: 470. https://doi.org/10.1186/s12872-024-04134-0.

[26] Sherzad AG, Shinwari M, Azimee MA, Nemat A, Zeng Q. Risk Factors for Calcific Aortic Valve Disease in Afghan Population. Vascular Health and Risk Management. 2022; 18: 643–652. https://doi.org/10.2147/VHRM.S376955.

[27] Livingstone R, Boyle JG, Petrie JR. How tightly controlled do fluctuations in blood glucose levels need to be to reduce the risk of developing complications in people with Type 1 diabetes? Diabetic Medicine: a Journal of the British Diabetic Association. 2020; 37: 513–521. https://doi.org/10.1111/dme.13911.

[28] Yapanis M, James S, Craig ME, O'Neal D, Ekinci EI. Complications of Diabetes and Metrics of Glycemic Management Derived From Continuous Glucose Monitoring. The Journal of Clinical Endocrinology and Metabolism. 2022; 107: e2221–e2236. https://doi.org/10.1210/clinem/dgac034.

[29] Ali MK, Pearson-Stuttard J, Selvin E, Gregg EW. Interpreting global trends in type 2 diabetes complications and mortality. Diabetologia. 2022; 65: 3–13. https://doi.org/10.1007/s00125-021-05585-2.

[30] Manduteanu I, Simionescu D, Simionescu A, Simionescu M. Aortic valve disease in diabetes: Molecular mechanisms and novel therapies. Journal of Cellular and Molecular Medicine. 2021; 25: 9483–9495. https://doi.org/10.1111/jcmm.16937.

[31] Lu Q, Lv J, Ye Y, Li Z, Wang W, Zhang B, *et al*. Prevalence and impact of diabetes in patients with valvular heart disease. iScience. 2024; 27: 109084. https://doi.org/10.1016/j.isci.2024.109084.

[32] Wong ND, Sattar N. Cardiovascular risk in diabetes mellitus: epidemiology, assessment and prevention. Nature Reviews. Cardiology. 2023; 20: 685–695. https://doi.org/10.1038/s41569-023-00877-z.

[33] Antar SA, Ashour NA, Sharaky M, Khattab M, Ashour NA, Zaid RT, *et al*. Diabetes mellitus: Classification, mediators, and complications; A gate to identify potential targets for the development of new effective treatments. Biomedicine & Pharmacotherapy = Biomedecine & Pharmacotherapie. 2023; 168: 115734. https://doi.org/10.1016/j.biopha.2023.115734.

[34] Han D, Zhou T, Li L, Ma Y, Chen S, Yang C, *et al*. AVCAPIR: A Novel Procalcific PIWI-Interacting RNA in Calcific Aortic Valve Disease. Circulation. 2024; 149: 1578–1597. https://doi.org/10.1161/CIRCULATIONAHA.123.065213.

[35] Lan NSR, Khan Z, Watts GF. Lipoprotein(a) and calcific aortic valve disease: current evidence and future directions. Current Opinion in Clinical Nutrition and Metabolic Care. 2024; 27: 77–86. https://doi.org/10.1097/MCO.0000000000000976.

[36] Anousakis-Vlachochristou N, Athanasiadou D, Carneiro KMM, Toutouzas K. Focusing on the Native Matrix Proteins in Calcific Aortic Valve Stenosis. JACC. Basic to Translational Science. 2023; 8: 1028–1039. https://doi.org/10.1016/j.jacbts.2023.01.009.

[37] Ballester-Servera C, Alonso J, Cañes L, Vázquez-Sufuentes P, Puertas-Umbert L, Fernández-Celis A, *et al*. Lysyl oxidase-dependent extracellular matrix crosslinking modulates calcification in atherosclerosis and aortic valve disease. Biomedicine & Pharmacotherapy = Biomedecine & Pharmacotherapie. 2023; 167: 115469. https://doi.org/10.1016/j.biopha.2023.115469.

[38] Di Vito A, Donato A, Presta I, Mancuso T, Brunetti FS, Mastroroberto P, *et al*. Extracellular Matrix in Calcific Aortic Valve Disease: Architecture, Dynamic and Perspectives. International Journal of Molecular Sciences. 2021; 22: 913. https://doi.org/10.3390/ijms22020913.

[39] Weinberg Sibony R, Segev O, Dor S, Raz I. Overview of oxidative stress and inflammation in diabetes. Journal of Diabetes. 2024; 16: e70014. https://doi.org/10.1111/1753-0407.70014.

[40] Ma XM, Geng K, Wang P, Jiang Z, Law BYK, Xu Y. MCT4-dependent lactate transport: a novel mechanism for cardiac energy metabolism injury and inflammation in type 2 diabetes mellitus. Cardiovascular Diabetology. 2024; 23: 96. https://doi.org/10.1186/s12933-024-02178-2.

[41] Tucureanu MM, Ciortan L, Macarie RD, Mihaila AC, Droc I, Butoi E, *et al*. The Specific Molecular Changes Induced by Diabetic Conditions in Valvular Endothelial Cells and upon Their Interactions with Monocytes Contribute to Endothelial Dysfunction. International Journal of Molecular Sciences. 2024; 25: 3048. https://doi.org/10.3390/ijms25053048.

[42] Deng H, Li H, Liu Z, Shen N, Dong N, Deng C, *et al*. Pro-osteogenic role of interleukin-22 in calcific aortic valve disease. Atherosclerosis. 2024; 388: 117424. https://doi.org/10.1016/j.atherosclerosis.2023.117424.

[43] Yoon D, Choi B, Kim JE, Kim EY, Chung SH, Min HJ, *et al*. Autotaxin inhibition attenuates the aortic valve calcification by suppressing inflammation-driven fibro-calcific remodeling of valvular interstitial cells. BMC Medicine. 2024; 22: 122. https://doi.org/10.1186/s12916-024-03342-x.

[44] Wu J, Huang H, Yang W, Xue T, Wang W, Zheng GD. TRPM4 mRNA stabilization by METTL3-mediated m6A modification promotes calcific aortic valve inflammation. Heliyon. 2024; 10: e31871. https://doi.org/10.1016/j.heliyon.2024.e31871.

[45] Yang X, Zeng J, Xie K, Su S, Guo Y, Zhang H, *et al*. Advanced glycation end product-modified low-density lipoprotein promotes pro-osteogenic reprogramming via RAGE/NF-κB pathway and exaggerates aortic valve calcification in hamsters. Molecular Medicine (Cambridge, Mass.). 2024; 30: 76. https://doi.org/10.1186/s10020-024-00833-8.

[46] Gong S, Xiang K, Chen L, Zhuang H, Song Y, Chen J. Integrated bioinformatics analysis identified leucine rich repeat containing 15 and secreted phosphoprotein 1 as hub genes for calcific aortic valve disease and osteoarthritis. IET Systems Biology. 2024; 18: 77–91. https://doi.org/10.1049/syb2.12091.